4660 *Chem. Mater.* **2010,** *22,* 4660–4668
DOI:10.1021/cm100837r

CHEMISTRY OF MATERIALS
Article

Ordered Mesoporous Boron Carbide Based Materials via Precursor Nanocasting

Lars Borchardt, Emanuel Kockrick, Philipp Wollmann, and Stefan Kaskel*

Department of Inorganic Chemistry Dresden University of Technology, Mommsenstrasse 6 D-01062 Dresden, Germany

Marta M. Guron and Larry G. Sneddon

Department of Chemistry University of Pennsylvania 231 South 34th Street Philadelphia, Pennsylvania 19104-6323

Dorin Geiger

Triebenberg Laboratory for HRTEM and Electron Holography Institute for Structure Physics, Dresden University of Technology, Zum Triebenberg 50 D-01328 Dresden, Germany

Received March 24, 2010. Revised Manuscript Received June 25, 2010

Ordered mesoporous boron carbide materials with high specific surface areas up to 778 m^2/g and hexagonal pore arrangement symmetries were obtained for the first time using a nanocasting strategy and the molecular bisdecaboranyl-hexane precursor for the infiltration into an ordered mesoporous silica template (SBA-15). Different preparation conditions were investigated, and it was found that by adjusting the precursor loading either nanorod structured replicas or tubular structured (CMK-5-like) materials were obtained. Changing the impregnation techniques, the solvents, and/or the pyrolysis temperatures allows tailoring of the properties of the hexagonal ordered mesoporous boron carbide replicas. The pore arrangement was altered to cubic ordered mesoporous boron carbide using KIT-6 silica matrix for nanocasting.

1. Introduction

Porous materials are of great interest in various applications. Their high surface areas and tunable pore sizes justify their use in catalysis, adsorption, separation, and sensing. The possibilities for synthesizing porous materials are numerous. However, since the first discovery of ordered mesoporous materials was reported in 1992, the interest in this new class of materials has grown significantly. Since then it has been possible to create highly porous silica materials with well-defined and controllable pore sizes in mesoscopic scales. They have been synthesized by a cooperative surfactant templating in aqueous systems. As useful as this pathway is, it excludes a lot of nonsiliceous materials, in particular nonoxides. The answer to this problem was a technique called nanocasting, which was reported for the first time by Ryoo et al. in 1999.[1] In a nanocasting process, a mold, called a template, is infiltrated with a precursor substance which is converted into the end product by pyrolysis, followed by a selective removal of the template. Because of this process, a replica can be obtained which corresponds to the inverse structure of the mold. Various nanomolds are reported in the literature. For example, zeolites,[2,3] carbons,[4] silicas,[1] alumina membranes,[5] or even larger structures like colloidal spheres[6] can be used as such hard templates.

The first material synthesized via this method was the ordered mesoporous carbon material CMK-1, with a cubic pore structure, resulting from the replication of the MCM-48 structure.[1] Other carbon replica structures were synthesized in hexagonally ordered SBA-15, with an ordered rodlike (CMK-3) or tubular replica structure (CMK-5). The space confined synthesis of metallic nanowires[7] and nanoparticles[8−10] has also been made possible using this nanocasting strategy. These mesoporous materials combine attractive qualities, like remarkably high specific surface areas, so far only known for microporous materials, with good diffusion properties and pore accessibilities,

*To whom correspondence should be addressed. Phone: 49-351-46333632. Fax: 49-351-46337287. E-mail: stefan.kaskel@chemie.tu-dresden.de.

(1) Ryoo, R.; Joo, S. H.; Jun, S. *J. Phys. Chem. B* **1999**, *103*, 7743–7746.
(2) Kyotani, T.; Nagai, T.; Inoue, S.; Tomita, A. *Chem. Mater.* **1997**, *9*, 609–615.
(3) Johnson, S. A.; Brigham, E. S.; Ollivier, P. J.; Mallouk, T. E. *Chem. Mater.* **1997**, *9*, 2448–2458.
(4) Schueth, F. *Angew. Chem., Int. Ed.* **2003**, *42*, 3604–3622.
(5) Martin, C. R. *Chem. Mater.* **1996**, *8*, 1739–1746.
(6) Velev, O. D.; Jede, T. A.; Lobo, R. F.; Lenhoff, A. M. *Nature* **1997**, *389*, 447–448.
(7) Shin, H. J.; Ko, C. H.; Ryoo, R. *J. Mater. Chem.* **2001**, *11*, 260–261.
(8) Kockrick, E.; Krawiec, P.; Schnelle, W.; Geiger, D.; Schappacher, F. M.; Pottgen, R.; Kaskel, S. *Adv. Mater.* **2007**, *19*, 3021–3026.
(9) Krawiec, P.; Kockrick, E.; Auffermann, G.; Simon, P.; Kaskel, S. *Chem. Mater.* **2006**, *18*, 2663–2669.
(10) Joo, S. H.; Choi, S. J.; Oh, I.; Kwak, J.; Liu, Z.; Terasaki, O.; Ryoo, R. *Nature* **2001**, *412*, 169–172.

Published on Web 07/14/2010

Scheme 1. Synthetic Route for the Preparation of Ordered Mesoporous Boron Carbide with Hexagonal Ordering of Mesopores

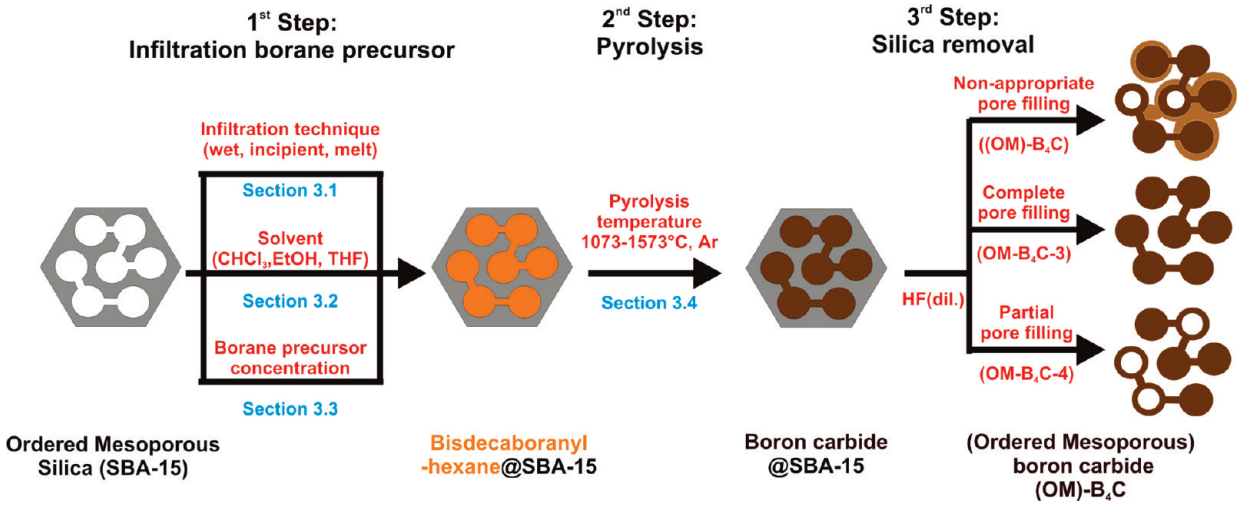

which are generally reserved for macroporous systems. Therefore, this new class of ordered mesostructured materials is promising for catalysis, sorption, and separation applications.[11−18] Especially, for catalytic processes at rigid conditions, adjusted material properties are necessary, like temperature stability or chemical inertness. However, there have been only a few studies of the syntheses of ordered mesoporous catalysts for high-temperature applications, such as nonoxide nitride and carbide ceramics.

The synthesis of ordered mesoporous silicon carbide materials[19,20] via this nanocasting route was introduced by Krawiec et al. with very high specific surface areas, well ordered pore structures, and narrow distributed pore sizes paired with a high temperature stability and chemical inertness of resulting replica material. The synthesis of ordered mesoporous boron carbide is particularly interesting owing to its high hardness, high temperature stability under inert atmosphere, and high resistance against oxidation in conjunction with low density (2.52 g/cm^3).[21] Thus, this nonoxide ceramic is attractive for various applications, such as blast nozzles, lightweight armor plates, wear resistance materials and in the nuclear industry as a neutron absorber or shield material caused by the large neutron absorption efficiency of boron atoms. With the combination of these attractive properties of boron carbide with those of an ordered mesoporous substance, a material can be created which can be applied as catalyst support for highly exothermic reactions at high temperatures. Typically, boron carbide can be prepared by carbothermal reduction of boron oxide in an electric arc-discharge furnace at 2473−2773 K. An alternative, more reliable method for the synthesis of boron carbide is the use of organic boron- and carbon-containing substances as precursors.[22−24] Sneddon et al. developed decaborane-based molecular and polymeric precursors and described the preparation of boron carbide nanofibers, nanocylinders, and nanoporous ceramics.[22,24−27]

In this study, one of these precursors (bisdecaboranyl-hexane) was used for precursor nanocasting to obtain mesoporous ordered boron carbides with hexagonal pore arrangement and high specific surface areas. This single source precursor has a boron/carbon ratio of 4:1.2, which is close to that of boron carbide (B_4C). The precursor gives a high ceramic yield and has a good solubility in a variety of organic solvents. Therefore, this molecular precursor was employed as a starting material in the nanocasting process for the preparation of ordered mesoporous boron carbide structures.

In the following, hexagonally ordered mesoporous silica (SBA-15) was impregnated under different conditions with the bisdecaboranyl-hexane precursor, followed by a pyrolysis under an inert atmosphere. The silica template was then desolved by hydrofluoric acid (Scheme 1). Different synthesis parameters, including different infiltration routes, organic solvents, precursor amounts, and pyrolysis conditions were studied. The optimized synthesis strategy was then also applied to synthesize the cubic boron carbide analogue by casting cubic ordered mesoporous silica (KIT-6).

(11) Corma, A. *Chem. Rev.* **1997**, *97*, 2373–2419.
(12) Schüth, F. *Chem. Mater.* **2001**, *13*, 3184–3195.
(13) Taguchi, A.; Schüth, F. *Microporous Mesoporous Mater.* **2005**, *77*, 1–45.
(14) Ying, J. Y.; Mehnert, C. P.; Wong, M. S. *Angew. Chem., Int. Ed.* **1999**, *38*, 56–77.
(15) Viswanathan, B.; Jacob, B. *Catal. Rev. Sci. Eng.* **2005**, *47*, 1–82.
(16) He, X.; Antonelli, D. *Angew. Chem., Int. Ed.* **2002**, *41*, 214–229.
(17) Soler-illia, G. J. D.; Sanchez, C.; Lebeau, B.; Patarin, J. *Chem. Rev.* **2002**, *102*, 4093–4138.
(18) On, D. T.; Desplantier-Giscard, D.; Danumah, C.; Kaliaguine, S. *Appl. Catal., A: General* **2001**, *222*, 299–357.
(19) Krawiec, P.; Geiger, D.; Kaskel, S. *Chem. Commun.* **2006**, 2469–2470.
(20) Krawiec, P.; Kaskel, S. *J. Solution Chem.* **2006**, *179*, 2281–2289.
(21) Thevenot, F. *Key Eng. Mater.* **1991**, *56−57*, 59–88.
(22) Pender, M. J.; Forsthoefel, K. M.; Sneddon, L. G. *Pure Appl. Chem.* **2003**, *75*, 1287–1294.
(23) Pender, M. J.; Wideman, T.; Carroll, P. J.; Sneddon, L. G. *J. Am. Chem. Soc.* **1998**, *120*, 9108–9109.
(24) Pender, M. J.; Sneddon, L. G. *Chem. Mater.* **2000**, *12*, 280–283.
(25) Welna, D. T.; Bender, J. D.; Wei, X.; Sneddon, L. G.; Allcock, H. R. *Adv. Mater.* **2005**, *17*, 859–862.
(26) Sneddon, L. G.; Pennder, M. J. (Trustees of the University of Pennsylvania, USA). Method for making boron carbide containing ceramics in the form of films, fibers, and nanostructured materials. US Patent 2000-539182-6478994 March 30, 2000.
(27) Mirabelli, M. G. L.; Sneddon, L. G. *J. Am. Chem. Soc.* **1988**, *110*, 3305–7.

2. Experimental Section

. All chemicals were used as received.

Synthesis of SBA-15[28]: A total of 8.1 g of Pluronic (EO_{20}-$PO_{70}EO_{20}$ P123, Aldrich) was dissolved in 146.8 g of deionized water and 4.4 g of concentrated HCl (37%) and stirred overnight at 308 K in a closed 250 mL one neck flask. To this solution, 16 g of TEOS (Aldrich 98%) was quickly added and stirred for 20 h at 308 K. The milky suspension was transferred to an autoclave and annealed at 403 K for 24 h. The solid product was filtered, washed with an HCl/water mixture, and calcined at 823 K.

Synthesis of KIT-6[29]: A total of 33.3 g of Pluronic (EO_{20}-$PO_{70}EO_{20}$ P123, Aldrich) was dissolved in 1204 g of deionized water and 65.8 g of concentrated HCl (37%) and stirred overnight at 308 K. To this solution, 33.3 g of *n*-butanol was added. After 1 h of stirring, 71.67 g of TEOS (Aldrich 98%) was quickly added and stirred for 20 h at 308 K. The milky suspension was transferred to an autoclave and annealed at 373 K for 24 h. The solid product was filtered, washed with an HCl/water mixture, and calcined at 823 K.

2.1. OM-B_4C Standard Synthesis (OM-B_4C-3). In a typical synthesis procedure, 0.273 g of the SBA-15 was infiltrated with 0.25 g of bisdecaboranyl-hexane precursor[23] solution in 20 mL of ethanol. The mixture was then left overnight for evaporation in a hood in an opened beaker, under constant stirring. The resulting powder was placed in an alumina boat in a tubular furnace under constant argon flow and then heated according to the following temperature program: (room temperature (RT) to 573 K at 150 K h^{-1}, then 5 h at 573 K, followed by heating to 973 at 30 K h^{-1}. After 973 K was reached, the sample was heated to the desired pyrolysis temperature (1273 K) at 120 K h^{-1} and maintained for 2 h). Afterward, the composite samples were dissolved in a mixture of EtOH/H_2O/40% HF (40 mL each), shaken, and left for 3 h for silica etching. Because of the dangerousness of hydrofluoric acid, these experiments were done in a separate flue. The solutions were then filtered over filter paper and washed with large amounts of EtOH (200 mL). The OM-B_4C materials were dried overnight in a hood (on the same filter) and then collected the next day.

2.2. OM-B_4C Synthesis (OM-B_4C-1; 2; 4−10). The other samples were prepared in analogy to section 2.1 with the following changes: OM-B_4C-1 was prepared via the incipient wetness method. The bisdecaboranyl-hexane precursor was dissolved in 7 mL of ethanol and was added dropwise to the SBA-15 template. As soon as the powder began to wet, it was put in a drying cabinet for 5 min. This procedure was repeated until all the precursor solution was dropped into the SBA-15.

OM- B_4C-2 was prepared via melt infiltration. The bisdecaboranyl-hexane precursor and SBA-15 were mixed together in a mortar and placed in a Schlenk-tube. The mixture was evacuated and flushed with argon three times, then heated to 473 K for 1 h. The mixture was cooled down, placed in an alumina boat, and treated according to the standard synthesis route (section 2.1). The synthesis of OM-B_4C-5 (OM-B_4C-6) followed the standard synthesis (section 2.1) with $CHCl_3$ (THF) as solvent. The synthesis of OM-B_4C-7 (8, 9) followed standard synthesis (section 2.1) with varied pyrolysis temperature of 1073 K (1423 and 1573 K). The synthesis of OM-B_4C-4 followed standard synthesis (section 2.1) but used half the amount of precursor. OM-B_4C-10 was synthesized according to OM-B_4C-1 but used 0.195 g of cubic KIT-6 silica instead of SBA-15.

2.3. Characterization. The low angle X-ray diffraction experiments were carried out in transmission mode on a Bruker Nanostar with Cu$K\alpha_1$ radiation (λ = 0.154 05 nm) and a position sensitive HiStar detector. Nitrogen physisorption isotherms were measured at 77 K using a Quantachrome Autosorb 1C apparatus. Prior to the measurement, the samples were activated in vacuum at 423 K for 24 h. Specific surface areas were calculated using the BET equation (p/p_o = 0.05−0.2). In order to evaluate the pore size distributions for boron carbide and silica composite materials, two methods were used: on the one hand the NLDFT equilibrium model (N_2 on carbon) based on cylindrical pores and on the other hand the Barrett−Joyner−Halenda (BJH) theory (adsorption branch). Because of the absence of density functional theory (DFT)-models for N_2 adsorption on boron carbide, the used N_2 on carbon-model does not reflect the fully correct pore size. Also the BJH theory should be handled with care in view of the fact that pores with diameter less than 5 nm are described. Transmission electron microscopy (TEM) investigations were performed on the Cs-corrected 200 kV-TEM FEI Tecnai F20 Cs-corr at the Triebenberg-Laboratory for high-resolution TEM and electron holography. The spherical aberration correction (Cs-correction) allowed a precise estimation of lateral dimensions avoiding errors due to delocalization effects. Elemental analyses using energy-dispersive X-ray spectroscopy (EDX) were obtained as a mean value of five measurements in a magnification of 3000. Carbon content was measured by high temperature combustion analysis (LECO C200) and oxygen content by hot extraction method (LECO TCH 600). Fourier transform-infrared (FT-IR) analysis was performed on a Nicolet Magna 550 series II instrument with OMNIC software. All measurements were carried out using diffuse reflection technique (PIKE EasyDiff), in combination with amorphous carbon-pads as the sample carrier, with 32 spectra averaged for each spectrum.

3. Results and Discussion

Ordered mesoporous boron carbide structures were prepared by the infiltration of molecular bisdecaboranyl-hexane precursor, followed by pyrolytic ceramic-conversion and finally silica removal by HF treatment (Scheme 1). In order to investigate the influence of the different synthesis conditions on the adsorption properties and mesoscopic ordering of resulting nonoxidic ceramic, the infiltration process (Scheme 1, step 1) was studied by varying the infiltration technique and the applied solvents. These results will be discussed in sections 3.1 and 3.2, respectively. The effect of pore filling degree of the molecular borane precursor inside the SBA-15 exo-template on the formation of mesoscopic ordered rodlike and tubular structures was studied (section 3.3). Additionally, the effect of different pyrolysis conditions (Scheme 1, step 2) on the preceramic composite system will be discussed for the optimized infiltration route in section 3.4. In order to study the modularity of this synthetic method, cubic boron carbide materials were prepared by infiltration into the KIT-6 exo-template (section 3.5).

3.1. Influence of the Infiltration Method on the Properties of Hexagonally Ordered OM-B_4C Materials Method. The ordered mesoporous boron carbide materials were prepared by the nanocasting strategy. Various methods have already been reported for the infiltration of molecular and polymeric precursor systems into exo-templates,

(28) Choi, M.; Heo, W.; Kleitz, F.; Ryoo, R. *Chem. Commun.* **2003**, 1340.
(29) Kleitz, F.; Choi, S. H.; Ryoo, R. *Chem. Commun.* **2003**, 2136–2137.

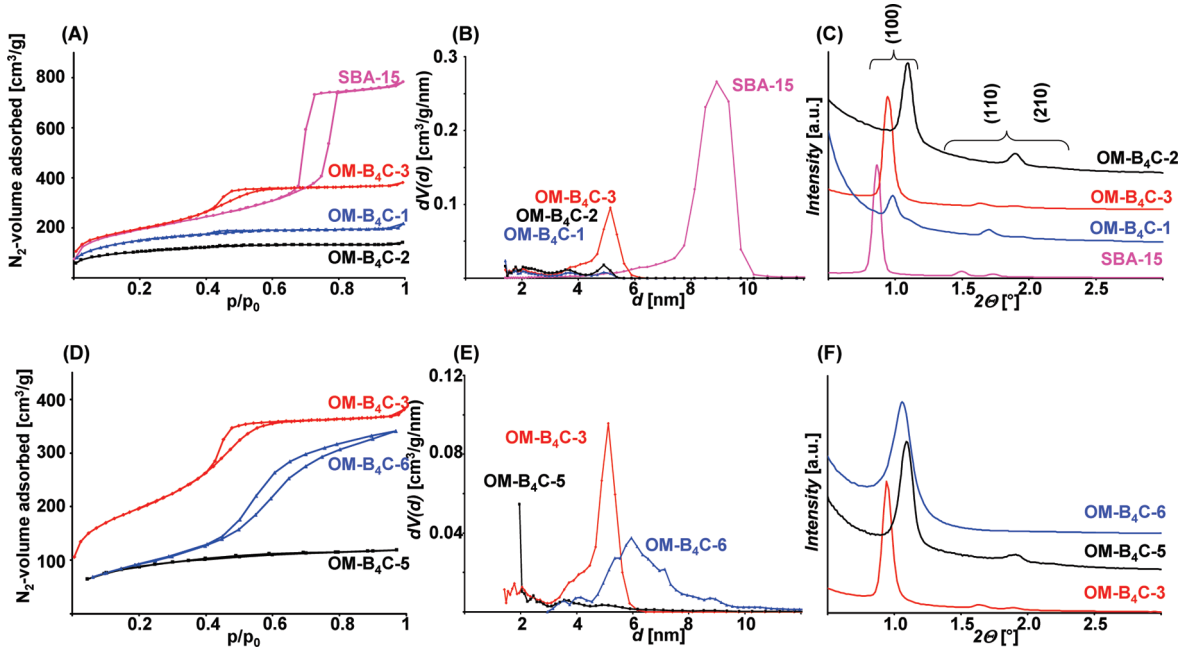

Figure 1. N_2-physisorption isotherms at 77 K (A, D), corresponding pore size distributions estimated by DFT model (B, E), and low angle X-ray diffraction patterns (C, F) of boron carbide replica structures prepared by different infiltration methods (A−C) and applied solvents (D−F), respectively.

with the method of choice depending on the properties of precursor material and the desired performance properties of the resulting replicas. In the present contribution, three different solvents and infiltration methods were explored for the infiltration of the molecular bisdecaboranyl-hexane precursor system into the pores of hexagonally ordered, mesoporous silica SBA-15. Borane precursor solutions dissolved in ethanol were infiltrated using the known incipient wetness and wet infiltration techniques.[19,30] Additionally, the melt infiltration method was studied, due to the temperature stability of the precursor.[23] The dry preceramic borane composite systems in the hexagonally ordered SBA-15 exo-template were pyrolyzed at 1273 K and the ceramic composites were subsequently treated with hydrofluoric acid in order to remove the silica matrix. The thermal treatment and leaching conditions were chosen according to the optimized OM-SiC synthesis strategy that was recently reported by our group.[19,30] The mesoscopic ordering and adsorption properties of the resulting boron carbide replica material were investigated by nitrogen physisorption measurements and low angle X-ray diffraction (Figure 1A−C). The adsorption properties were strongly dependent on the infiltration route. The boron carbide materials prepared by the incipient wetness and melt infiltration techniques had significantly lower specific surface areas and pore volumes compared to that synthesized by wet infiltration with 705 m^2/g and 0.57 cm^3/g. The latter results can be explained by inhomogeneous pore filling, resulting local precursor oversaturation, and incomplete filling, respectively, because of the fast evaporation of the applied solvent (incipient wetness method) and the nucleation of the borane precursor at higher temperatures (melt infiltration). Thus, only a reduced ratio of the molecular precursor was precipitated inside the pores of hexagonally ordered pores with the remaining amount located on the outer surface or forming separate solid structures (Scheme 1). During the subsequent thermal treatment and leaching processes, nonporous layers and (nanoscale) bulk structures were formed. Additionally, because of the partial pore filling, the resulting nanoparticular and tubular structures showed less stability toward sintering and agglomeration processes causing pore blocking effects (Scheme 1). This assumption was confirmed by both the lower surface areas by the isotherm shape and the pore size distributions calculated by appropriate BJH (Figure 3A) and nonlocal density functional theory (NLDFT) methods (Figure 1B) of the ceramic nanocast materials. In contrast to the characteristic type IV isotherm shape of OM-B_4C-3, which had a narrow pore size distribution in the mesopore range, the incipient wetness (OM-B_4C-1) and melt methods (OM-B_4C-2) methods yielded mainly microporous materials with pore sizes less than 2 nm. A mean pore diameter of 3.7 nm (BJH) and 5.1 nm (NLDFT) were observed for the OM-B_4C-3 replica prepared by wet infiltration, while broad distributions were obtained for materials synthesized by the other infiltration methods.

All nanocast materials showed mesoscopic ordering since the characteristic (100) and (110) peaks were detected. In comparison to the SBA-15 exo-template, the peaks of the replica materials were shifted to higher diffraction angles and the corresponding lattice constants were reduced from 11.9 (SBA-15) to 10.8 nm (OM-B_4C-3). The latter decrease is typical of many nanocast materials[31] and can be explained by sintering taking place at high temperatures during the thermal treatment processes. However, all peaks of the starting silica material were also

(30) Krawiec, P.; Schrage, C.; Kockrick, E.; Kaskel, S. *Chem. Mater.* **2008**, *20*, 5421–5433.

(31) Lu, A. H.; Schueth, F. *Adv. Mater.* **2006**, *18*, 1793–1805.

Table 1. OM-B_4C Materials Synthesized by Nanocasting of Bisdecaboranyl-Hexane in a Hexagonally Ordered Mesoporous Silica Matrix under Different Conditions

sample code OM-B_4C-	infiltration method[a]	solvent	$T_{Pyrolysis}$ [K]	S_g[b] [m^2/g]	V_{pore}[c] [cm^3/g]	d_{Pore}[d] [nm]	a[e] [nm]
SBA-15				702	1.18	8.8	11.9
KIT-6				600	1.29	10.2	23.0
1	I.W.	EtOH	1273	546	0.31	4.9 weak	10.4
2	melt		1273	373	0.2	4.9 weak	9.3
3	wet	EtOH	1273	705	0.57	5.1	10.8
4[f]	wet	EtOH	1273	725	0.56	2.4/3.9/5.1	10.2
5	wet	$CHCl_3$	1273	293	0.18	3.6 weak	9.4
6	wet	THF	1273	394	0.53	6.0 broad	9.5
7	wet	EtOH	1073	778	0.65	5.1	10.6
8	wet	EtOH	1423	500	0.53	5.0/6.0	8.9
9	wet	EtOH	1573	48	0.12		
10[g]	wet	EtOH	1073	591	0.53	4.6	21.4

[a] I.W., incipient wetness; melt, melt infiltration; wet, wet infiltration. [b] S_g estimated at $p/p_0 = 0.05-0.2$. [c] Total pore volume calculated at $p/p_0 = 0.95$. [d] Pore diameter calculated by NLDFT methods for cylindrical pores at 77 K for silica with adsorption model and for B_4C replica structures using carbon kernel. [e] Lattice constants estimated of 100 peak for 2D hexagonal pore systems and of (210) peak for the cubic pore system. [f] 50% pore filling degree of bisdecaboranyl-hexane related to the specific pore volume of SBA-15 exo-template. [g] Cubic ordered KIT-6 as exo-template for nanocasting process.

detectable for the OM-B_4C-3 replica material, with the similar peak intensity ratios suggesting the formation of rodlike structures comparable to ordered mesoporous carbonaceous CMK-3 and ceramic SiC-3[1,30] materials. Infrared spectroscopic investigations (Figure 7A) confirmed the formation of boron carbide with all three infiltration methods (see Table 2 for peak identification). For all samples, a weak B−H absorption at 2510 cm^{-1} was observed along with B−O impurities at 1420 cm^{-1}. These impurities result from air oxidation at ambient conditions but also could arise from reactions at the B_4C/SiO_2 interface during pyrolysis. These impurities were reduced with repeated HF-washing of the samples. Figure 7D shows the decreased B−O band, compared to that of the OM-B_4C-3 as synthesized (1× HF), following a three- and six-time washed OM-B_4C-3. The small C−H (2930 cm^{-1}) and O−H (3400 cm^{-1}) absorptions can be assigned to ethanol adsorption during the washing process. An additional possible side-reaction in the nanocasting process is the reaction of the boron-precursor with the SBA-matrix, but apart from a small Si−O absorption at 1110 cm^{-1}, no Si−C bands were detected in the spectra. Only very weak contributions to the background of some spectra are possible. Thus, the infrared investigations indicate the formation of a nearly silica-free material with only a few oxygen-impurities.This conclusion is also confirmed by elemental analysis.

3.2. Solvent Influence on the Properties of Hexagonally Ordered OM-B_4C materials. The previous section demonstrated that the wet infiltration technique using an ethanolic borane precursor solution was the best method for the synthesis of high-quality boron carbide materials (OM-B_4C-3). In the following section, the influence of the solvent on the ordering and adsorption properties of the ceramic replica will be discussed. Diverse solvents such as chloroform, tetrahydrofuran, and ethanol were chosen

Table 2. Peak Identification of FT-IR Spectra

wavenumbers [cm^{-1}]	classification	ref
1110	ν (Si−O)	33
1151	ν (B−C)	34
		35
1214	ν (B−C)	33
		35
1360	δ (O−H)	36
1420	ν (B−O)	33
		35
1625	ν (C−B−C)	37
		38
1735	instrument peak[a]	
2510	ν (B−H)	33
		39
2950 ... 2850	ν (C−H)	36
		39
3400	ν (O−H)	36
		35

[a] This peak is caused by the used diffuse reflection technique and could not be removed with background spectra.

because of their different polarity and vapor pressure. According to the isotherms in Figure 1D, the adsorption properties were strongly dependent on the applied solvents. The B_4C ceramics prepared from chloroform solutions (OM-B_4C-5) were completely microporous with moderate specific surface areas and pore volumes of 293 m^2/g and 0.18 cm^3/g, respectively. Ceramics prepared from THF solvent (OM-B_4C-6) gave replica materials with larger pore volumes of 0.53 cm^3/g due to the presence of mesopores in the range of 6 nm. Nevertheless, the specific surface area of 394 m^2/g was significantly lower compared to the material prepared by infiltration of the ethanolic solution with 705 m^2/g (OM-B_4C-3). These results can be explained by the polarity and the vapor pressure of applied solvents in relationship to the polar inner surface SBA-15 template. Since chloroform is hydrophobic, there should only be weak interactions with the silanol groups of the silica matrix. In contrast, a good surface wetting of hydrophilic ethanol solution on the silica support can be expected. Additionally, the vapor pressure of the chlorinated solvent was significantly higher than those of EtOH and THF, causing a higher rate of unintentional precipitation of the borane precursor outside the pores of SBA-15. The latter could explain the lower specific surface area and pore volume of OM-B_4C-5 compared to the ether and alcohol solution derived replica materials. Also, the broader pore size distribution (Figures 1E and 3B) and lower specific surface area of the THF solution prepared OM-B_4C-6 can

(32) Krawiec, P.; Kockrick, E.; Borchardt, L.; Geiger, D.; Corma, A.; Kaskel, S. *J. Phys. Chem. C* **2009**, *113*, 7755–7761.
(33) Postel, O. B.; Heberlein, J. V. R. *Diamond Relat. Mater.* **1999**, *8*, 1878–1884.
(34) Sun, J.; Ling, H.; Pan, W. J.; Xu, N.; Ying, Z. F.; Shen, W. D.; Wu, J. D. *Tribol. Lett.* **2004**, *17*, 99–104.
(35) Mondal, S.; Banthia, A. K. *J. Eur. Ceram. Soc.* **2005**, *25*, 287–291.
(36) Steger, W. E.; Dathe, K.; Herzschuh, R.; Mehlhorn, A.; Müller, B.; Müller, E. *Strukturanalytik*; Deutscher Verlag für Grundstoffindustrie GmbH: Leipzig, Stuttgart, Germany , 1992.
(37) Kuhlmann, U.; Werheit, H.; Schwetz, K. A. *J. Alloys Compd.* **1992**, *189*, 249–258.
(38) Shirai, K.; Emura, S.; Gonda, S.-i.; Kumashiro, Y. *J. Appl. Phys.* **1995**, *78*, 3392.
(39) Braddock-Wilking, J.; Lin, S.-H.; Feldman, B. *Tribol. Lett.* **1998**, *5*, 145–148.

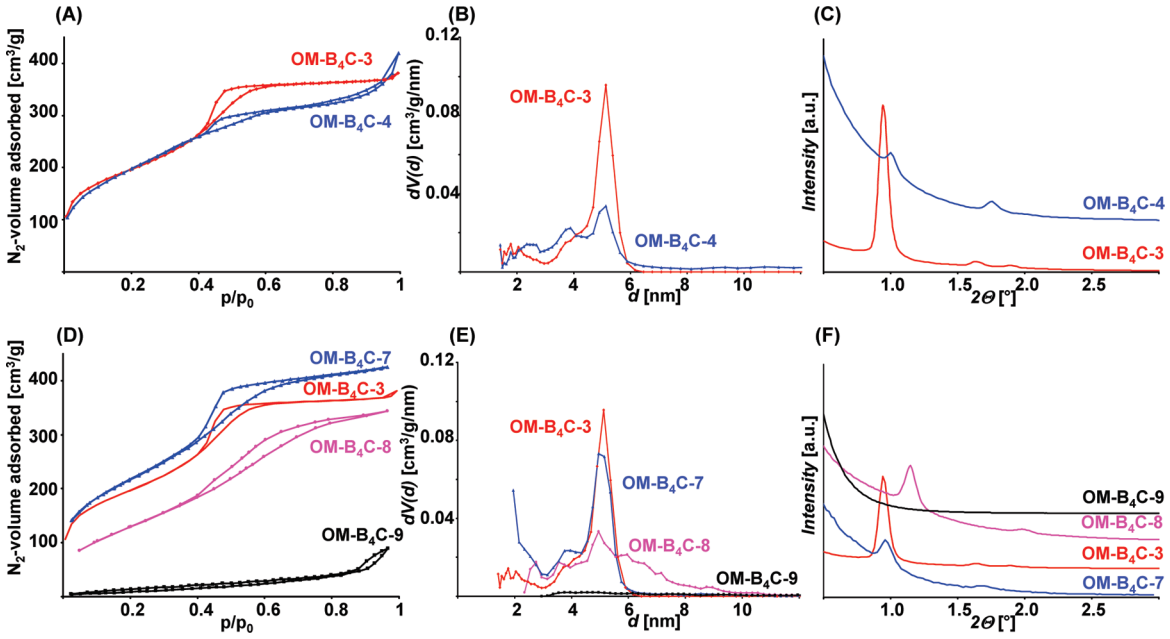

Figure 2. N_2-physisorption isotherms at 77 K (A, D), corresponding pore size distributions estimated by the DFT model (B, E), and low angle X-ray diffraction patterns (C, F) of boron carbide replica structures prepared by different borane precursor amounts (A−C) and pyrolysis temperatures (D−F), respectively.

be attributed to the lower boiling point of THF (331 K) compared to ethanol (351 K).

The low-angle X-ray diffraction patterns confirmed the mesoscopic ordering of the boron carbide ceramics (Figure 1F). However, materials prepared using the ethanolic solution (OM-B_4C-3) had larger lattice constants. This indicates a lower degree of sintering during the pyrolysis process that can be attributed to the higher degree of pore filling using ethanolic solutions. This was verified by the results of nitrogen physisorption measurements that were discussed earlier.

The IR-spectroscopic analysis in Figure 7B confirmed the formation of boron carbide for each of the ethanol, tetrahydrofuran, and trichloromethane solvents with the peak identifications given in Table 2 and section 3.1. As can be seen in the spectra, complete precursor ceramic-conversion was observed in all three solvents. The product spectra agree well with the spectrum of bulk B_4C (Aldrich, 99%).

3.3. Influence of the Amount of Infiltrated Precursor on the Properties of Hexagonally Ordered OM-B_4C Materials. The influence of different pore filling degrees of the borane precursor solution on the structural and adsorption properties of the resulting boron carbide ceramic were also investigated. According to the previous results, an ethanolic borane solution was infiltrated by the wet infiltration method with a lower, theoretical pore filling degree of 50%. The composite treatment was performed under similar conditions to already introduced replica material (OM-B_4C-3) with quantitative pore filling. The nitrogen physisorption isotherms and the corresponding pore size distributions estimated by classical BJH and quantum mechanical DFT theory of the boron carbide replica materials prepared by partial (OM-B_4C-4) and complete pore filling (OM-B_4C-3) degree are presented in Figures 2A,B and 3C, respectively. Both materials exhibit characteristic type IV isotherm shapes with similar high specific surface areas in the range of 700 m^2/g and pore volumes of 0.57 cm^3/g. However, there were significant differences in pore size distributions for the replica materials. The OM-B_4C-3 replica had a monomodal pore diameter with 3.7 nm (BJH) and 5.1 nm (DFT), respectively. In contrast, the OM-B_4C-4 replica with the lower pore filling degree showed a broader distribution with additional maxima at lower diameters. The peak with a diameter of 3.9 nm corresponds to the pore system P_1, which describes the interspaces between the B_4C rods. The smaller peak maxima corresponds to the internal pore-system P_2 with different pore diameters. It is assumed that a partial infiltration of precursor into the mesoporous system of the silica led to simply coating of the pore walls, producing a tubular and CMK-5 like structure with a bimodal pore size distribution.

The ordered pore structure of boron carbide replica was also confirmed by transmission electron microscopy presented in Figure 4. Both the material with partial and quantitative pore filling had the characteristic ordered pore arrangement (Figure 4B,D) that has already been observed for a variety of replica materials prepared by a SBA-15 exo-template.[31]

3.4. Influence of the Pyrolysis Temperature on the Properties of Hexagonally Ordered OM-B_4C Materials. Previous studies on the synthesis of ordered mesoporous silicon (oxy)carbide structures identified the pyrolysis temperature as a fundamental parameter affecting the replica properties.[19,20,30] Therefore, the influence of different pyrolysis temperatures over the 1073−1573 K range on the boron carbide system was studied. According to the results of nitrogen physisorption measurements, the specific surface area as well as the total pore

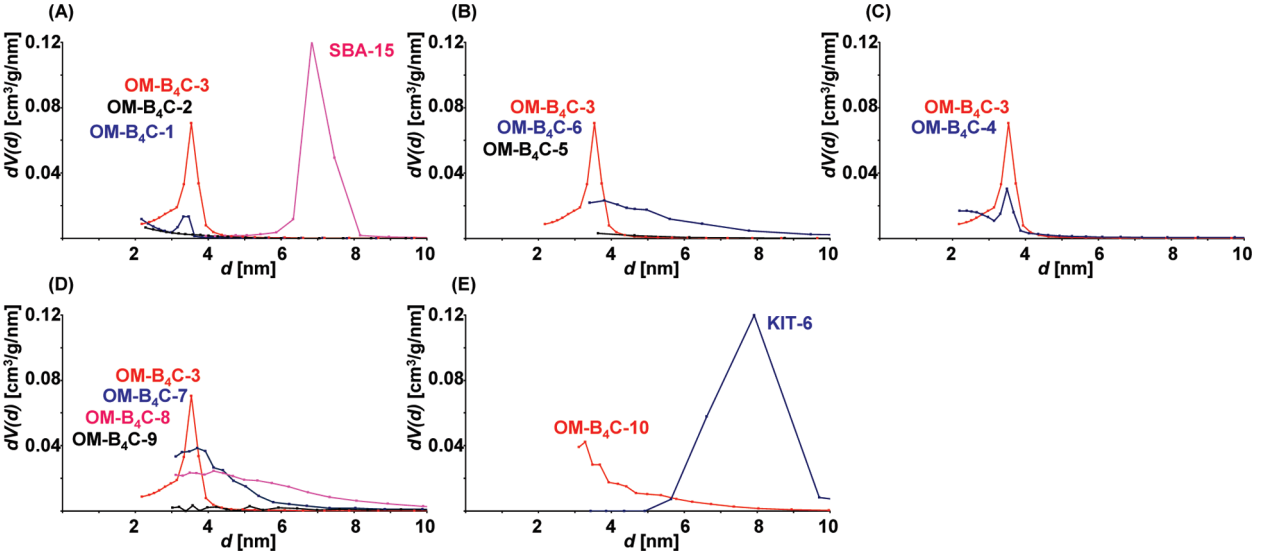

Figure 3. Pore size distribution estimated from the adsorption branch using BJH theory. OM-B_4C were synthesized (A) with different infiltration technique, (B) with different solvents, (C) with different amounts of infiltrated precursor, (D) with different pyrolysis temperature, and (E) in a silica template with cubic pore structure.

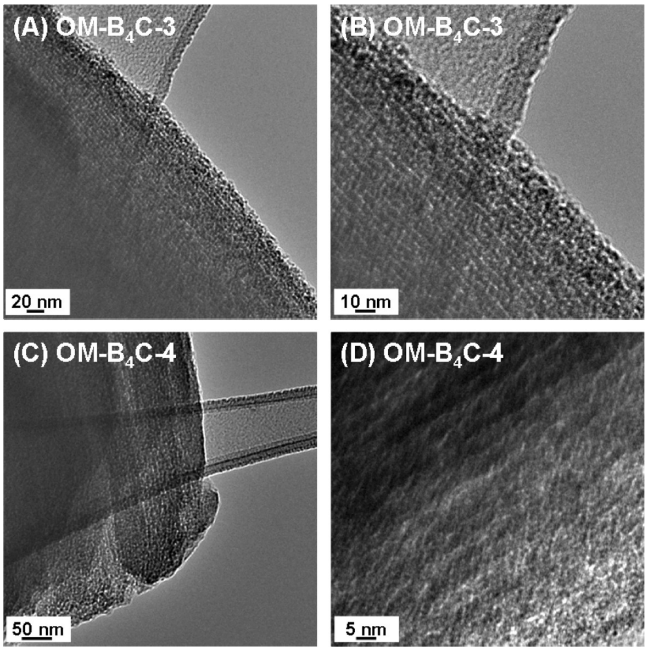

Figure 4. Transmission electron micrographs of ordered mesoporous boron carbide structures synthesized by incipient wetness infiltration of quantitative (OM-B_4C-3) and semiquantitative amounts (OM-B_4C-4) of borane precursor.

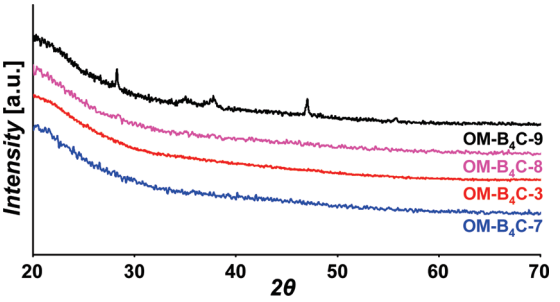

Figure 5. X-ray powder diffraction pattern of boron carbide replica structures pyrolyzed at 1073−1573 K.

volume decreased from 778 to 500 m^2/g and from 0.65 to 0.53 cm^3/g, respectively, when the temperature was raised from 1073 K (OM-B_4C-7) to 1423 K (OM-B_4C-8). In addition, the lattice constant reduced from 10.7 to 8.9 nm, indicating stronger sintering at the higher pyrolysis temperatures. Similar effects were also observed for silicon carbide systems.[32] However, comparable maxima in pore size distributions of approximately 5 and 4 nm were calculated by the DFT and BJH methods after pyrolysis at 1073−1423 K. Nevertheless, a broader distribution resulted for the material treated at 1423 K (OM-B_4C-8). The latter can be attributed to crystallization processes increasing the density of the nonoxide ceramic, as confirmed by wide-angle X-ray diffraction (Figure 5).

Materials pyrolyzed at 1573 K showed no significant porosity and mesoscopic ordering since the materials had only 48 m^2/g and no characteristic peaks in the low angle area. This can be attributed to partial crystallization at this temperature, since the characteristic peaks of the rhombohedral B_4C phase are detectable (OM-B_4C-9). Only X-ray amorphous ceramic materials resulted after pyrolysis at lower temperatures. However, additional peaks of OM-B_4C-9 indicate the formation of a second crystalline phase. The latter results were also verified by elemental analysis, which showed high oxygen and silicon contents up to 26 wt % and 14 wt %, respectively. Nevertheless, smaller amounts of these elements were also detected for replica materials prepared at lower pyrolysis temperatures. In order to reduce the silicate content, multiple HF treatment processes up to six times were used. The silicate as well as the oxygen amount could be reduced to 5 wt % and 9 wt %, respectively, for OM-B_4C-3. Oxycarbide formation was also previously observed in mesoporous SiC replica structures and was attributed to surface passivation processes.[30] Trace silicon could still be detected after multiple HF treatments, suggesting the formation of ternary silicide or quaternary silicate compositions. These results can be

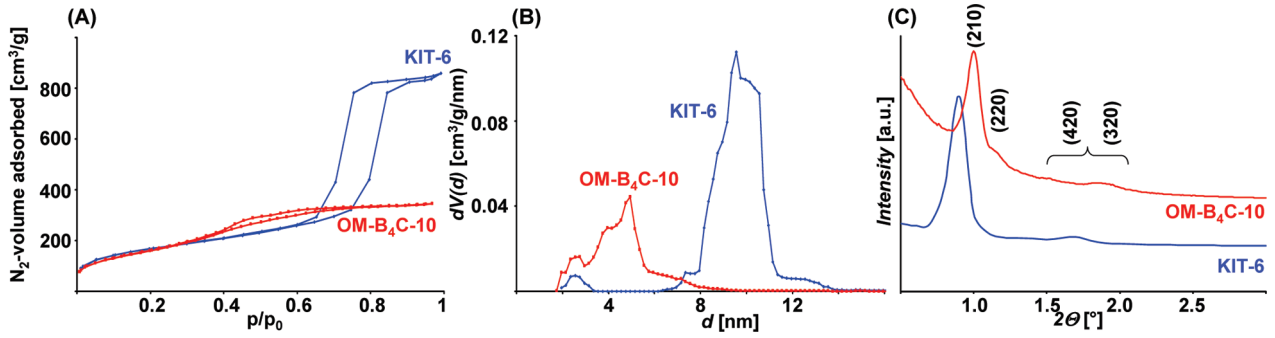

Figure 6. N_2-physisorption isotherms at 77 K (A), corresponding pore size distributions estimated by the DFT model (B), and low-angle X-ray diffraction patterns (C) of boron carbide replica structures prepared in cubic KIT-6 exo-template.

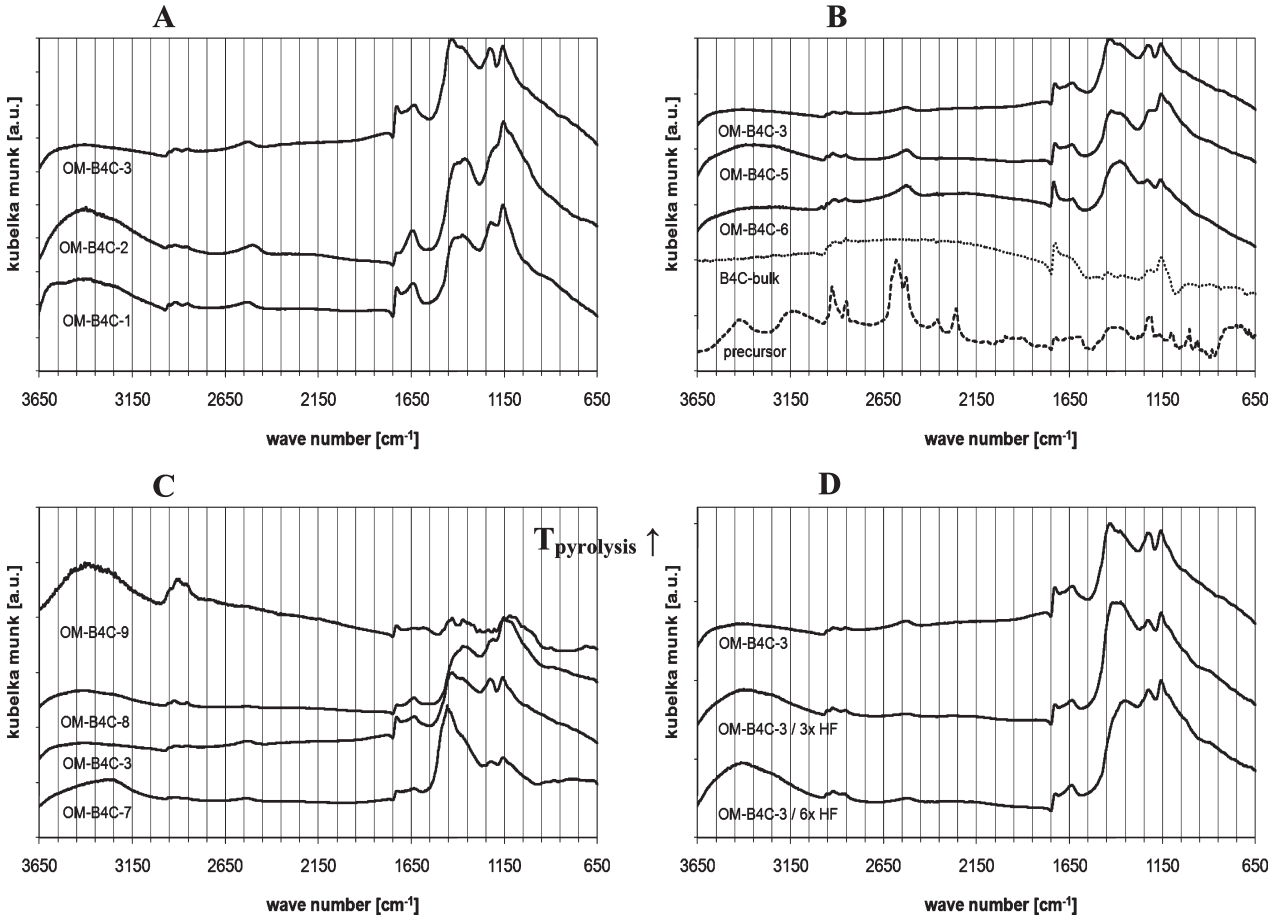

Figure 7. FT-IR spectra of OM-B_4C samples synthesized with different infiltration methods (A), with different solvents in comparison with bisdecaboranylhexane and a commercially available nonporous reference B_4C sample (B), and with different pyrolysis temperatures (C) and repeated washings in HF (D).

explained by diffusion processes at the interface of the silica matrix (SBA-15) and the nonoxide ceramic at elevated temperatures.

The elemental analysis results are supported by the infrared-spectroscopic investigations (Figure 7C) of samples synthesized in ethanol from 1073 K up to 1573 K. At the lower synthesis temperature of 1073 K, significant formation of B−O bonds was indicated by the peak at 1420 cm^{-1} (refer to Table 2 for peak assignment and section 3.1), whereas the formation of B_4C was lowered. When the synthesis temperature was higher than 1300 K, increased formation of Si−O was observed, as indicated by the peak at 1110 cm^{-1} and the (Si−O)/(B−C) peak ratio. The best result, as seen in Figure 7C, was achieved for the sample synthesized at 1273 K. As mentioned before, the remaining B−O impurities were reduced by multiple HF-washing cycles (Figure 7D). The adsorption measurements indicated that these treatments produced a highly porous and nearly pure B_4C material.

A batch of OM-B_4C was prepared, divided, and pyrolyzed at various temperatures. According to low angle X-ray diffraction, all samples, except OM-B_4C-9 (1573 K pyrolysis), showed characteristic peaks for the hexagonal ordered replica structure (Figure 2F). The synthesis at

1573 K (OM-B_4C-9) resulted in totally disordered structures and a collapse of the porous system. Furthermore, the replica and template could not be separated with hydrofluoric acid after pyrolysis. Therefore, there is evidence for the formation of mixed phases between the boron carbide and the silica out of the matrix.

Figure 2F demonstrates that the peaks in the low angle-XRD (especially the [100]) are shifted to higher 2Θ angles for materials pyrolyzed at higher temperature. This decrease of the lattice constant indicates that the pore system collapses with higher temperature continuously. The N_2-physisorption (Figure 2D) data support this interpretation. OM-B_4C-7 had a specific surface area up to 778 m^2/g and a specific pore volume up to 0.65 cm^3/g. By pyrolysis at higher temperatures, both the pore volume and the surface area decreased until the mesoporous and ordered system completely collapsed (OM-B_4C-9). The pore size distributions (DFT) of samples synthesized between 1073 and 1423 K are shown in Figure 2E. It was further investigated whether a post-treatment of the OM-B_4C samples at higher temperature caused crystallization. Samples were treated at 1773 K in argon flow for 3 h. High angle-X-ray diffraction showed nanocrystalline character for those samples but a loss of ordering and porosity. Thus, a compromise has to be found for porosity on the one hand and crystallinity on the other hand.

3.5. Synthesis of Cubic Ordered Mesoporous Boron Carbide Structures. In order to demonstrate the modular synthesis strategy for the nanocasting method, ordered mesoporous boron carbide structures were synthesized in cubic ordered silica KIT-6. The optimized wet infiltration method in ethanol and subsequent thermal treatment at 1073 K were used as described in the previous sections. The resulting replica material presented in Figure 6 showed the characteristic mesoporous isotherm shape with a narrow pore size distribution in the range of 4.6 nm. The estimated specific surface area and total pore volume of 591 m^2/g and 0.53 cm^3/g are comparable to those synthesized in hexagonally ordered exo-template (Table 1). However, replica structures synthesized in KIT-6 had a higher degree of mesoscopic ordering, since beside the 210 peak also the 210 and 400 peaks are detectable (Figure 6C). The latter suggests a homogeneous pore filling of the applied borane precursor inside the cubic KIT-6 matrix. Nevertheless, the lattice constants of the replica structures slightly decreased compared to the ordered mesoporous silica structure caused by sintering effects that were already discussed in the previous sections. Ordered mesoporous pore structure of OM-B_4C-10 were also confirmed by TEM investigations presented in Figure 8.

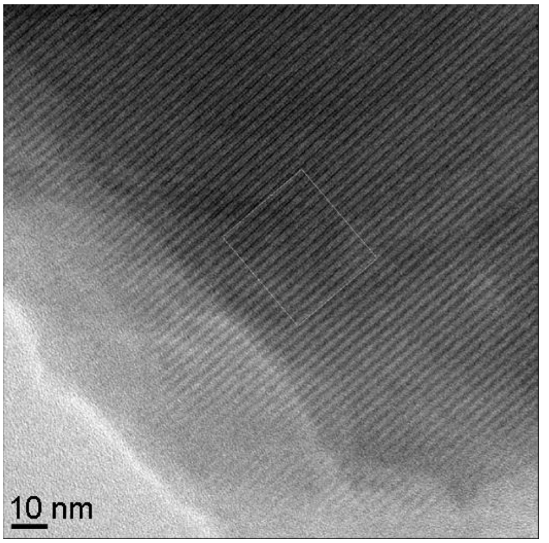

Figure 8. Transmission electron micrograph of cubic ordered mesoporous boron carbide (OM-B_4C-10).

Conclusions

In this paper, hexagonally and cubic ordered mesoporous boron carbide materials were successfully synthesized by nanocasting method for the first time. We investigated the influence of different preparation conditions. We have shown that wet-infiltration causes a homogeneous filling of the pore system of the template, resulting in a highly ordered and porous replica structure. Furthermore, we showed the significant influence of the solvent on the building of an ordered mesoscopic structure. In addition, the influence of the pyrolysis temperature was investigated resulting in OM-B_4C synthesized at 1073 K with the highest specific surface area (778 m^2/g). The increase of temperature led to decreasing surface areas and pore volume but also resulted in nanocrystalline material with a lower oxygen content.

Note Added after ASAP Publication. There was an error in the presentation of the names of the authors in the version published ASAP July 14, 2010; the corrected version was published ASAP July 30, 2010.

Supporting Information Available: Thermogravimetric measurement of OM-B_4C under synthetic air and under argon 5.0 atmosphere (PDF). This material is available free of charge via the Internet at http://pubs.acs.org.